Spatial Dependence of Exchange Interaction in Heisenberg Antiferromagnet $Zn_{1-x}Mn_xTe$

Qun Shen
Cornell High Energy Synchrotron Source, Cornell University, Ithaca, New York 14853

H. Luo,* and J. K. Furdyna
Department of Physics, University of Notre Dame, Notre Dame, Indiana 46556
(Received 7 March 1995)

X-ray diffraction study of exchange striction in a $Zn_{1-x}Mn_xTe$ [001] epilayer reveals a long-ranged magnetic exchange interaction. A new *independent-exchange-path* model is proposed to explain the experimental result. It provides the strengths of exchange constants for all neighboring spins.

PACS numbers: 75.30.Et, 75.50.Ee, 75.60.Ch, 78.70.Ck

Magnetic ordering in a crystal lattice is determined by the properties of an exchange interaction between a pair of spins, $\mathbf{S}_i$ and $\mathbf{S}_j$, as described by the well-known Heisenberg Hamiltonian [1], $H_{ex} = -2\sum J(r)\mathbf{S}_i \cdot \mathbf{S}_j$, where $J(r)$ is the exchange parameter and r is the spatial separation of the two spins. Studies of the exchange constant $J(r)$ and its dependence on the spatial separations of neighboring spins represent an important aspect of solid state physics in magnetic materials.

For manganese-containing zinc-blende alloys, also known as diluted magnetic semiconductors (DMS's), an antiferromagnetic (AFM) nearest-neighbor (NN) Mn-Mn exchange (described by J_1) dominates the spin interactions, and results in a type-III AFM order at low temperatures [2] in the face-centered-cubic (fcc) lattice. The magnetic structures of these materials have been studied extensively by elastic neutron scattering [3], and the NN exchange integrals J_1 have been measured using such techniques as high-field magnetization steps [4] and inelastic neutron scattering [5,6]. Very little is known, however, about the spatial variation of the exchange constant $J(r)$ and, consequently, about the strengths of the more-distant-neighbor interactions. Theoretically, it has been shown [7] that superexchange is the predominant exchange mechanism in DMS materials, but many fundamental questions about $J(r)$ remain [8–11]. One such basic question is whether the interaction is of short-range or of long-range nature. The short-range behavior is derived by Larson *et al.* [7] from a three-level theoretical model, which yields an isotropic spatial dependence of $J(r)$ in the Gaussian form $\exp(-\beta r^2/a^2)$, where $\beta = 4.89$ and a is the fcc lattice constant. A longer-range interaction of a form $J(r) \sim (r/a)^{-n}$, with $n \approx 5$–7, has been proposed by Twardowski *et al.* [12], based on an empirical analysis of low-temperature susceptibility data, together with the assumption that the Mn ions are distributed in a completely random fashion. A much weaker spatial dependence for the second through the fourth nearest-neighbor constants is suggested by Bruno and Lascaray [13], based on the number of equivalent ways of connecting these distant neighbors through the anion-cation chemical bonds. Available experimental estimates on the distant-neighbor exchange constants are generally indirect and imprecise, making it difficult to distinguish these existing models [8,9].

One of the most direct ways to obtain the spatial dependence of the exchange interaction is to measure the lattice distortions (*exchange striction*) in the magnetically ordered phase by x-ray diffraction [14,15]. In this Letter we utilize this effect to study the Mn exchange interactions in a type-III fcc DMS epilayer $Zn_{1-x}Mn_xTe$. Our results reveal a long-ranged exchange interaction, which leads to a new model of the spatial and the directional dependence of the superexchange interaction in DMS materials. Our model accounts for all neighboring interactions, and shows a predominant NN exchange as well as a long-ranged interaction among the distant neighbors.

The $Zn_{1-x}Mn_xTe$ sample used in our study was a 1 μm thick specimen with $x = (93.8 \pm 0.5)\%$, grown by molecular beam epitaxy (MBE) on a GaAs(001) substrate, with a 2 μm ZnTe buffer layer to minimize the lattice mismatch [16]. The crystal structure of $Zn_{1-x}Mn_xTe$ is of the zinc-blende type, with $a = 6.323$ Å. The x-ray measurements were performed at the A2 station of Cornell High Energy Synchrotron Source (CHESS), with an incident x-ray energy of 18 keV. The sample temperature was controlled to ± 1 K by a closed-cycle helium refrigerator, which was mounted on a standard 4-circle diffractometer. A perfect-crystal analyzer was used for high resolution lattice parameter measurements, which provides a precision of $\Delta a/a \approx 3 \times 10^{-5}$. Although there is considerable lattice mismatch between the $Zn_{1-x}Mn_xTe$ epilayer and the buffer, our measurements of the lattice constants normal and parallel to the growth plane showed an almost strain-free $Zn_{1-x}Mn_xTe$ epitaxial layer, indicating that the epilayer was sufficiently thick to relax to an essentially cubic high-temperature phase.

At temperatures below the Néel temperature $T_N = 62$ K, the $Zn_{1-x}Mn_xTe$ layer exhibits type-III AFM order, with the unit cell doubled along the cubic axes ([001], [010], and [100]), creating three types of equivalent domains in different regions of the sample

 0031-9007/95/75(13)/2590(4)$06.00

[16]. The magnetic ordering is accompanied by the exchange striction effect, causing a Bragg reflection to split into two (or more) peaks. In order to obtain complete information on the lattice distortions in the different domains, we measured several Bragg reflections in different crystallographic directions at low temperatures. In Fig. 1 we show a typical splitting of the (208) and (802) Bragg reflections at $T = 25$ K (filled circles), with the corresponding $T = 55$ K profiles as dashed lines. The temperature dependence of the splitting, converted to the lattice constants parallel and normal to the epilayer plane, is shown in the inset in each plot. It shows that the exchange striction effect occurs at around 52 K, which is well below the Neél temperature of 62 K. This result confirms earlier measurements on MnTe thin films [16], and we will come back to this "delayed" magnetostriction phenomenon below.

Figure 1 shows that the [100] and [010] domains (those with cell-doubling axes in the epilayer plane), although equivalent to each other, are not equivalent to the [001] domains. A quantitative analysis on the peak intensities and positions indicates that (i) at the lowest temperatures the [001] type comprises about 60% of the domain population, while the [100] and [010] types share the remaining 40%; and (ii) the [001] domains are *tetragonally* deformed, but the [100] and [010] domains are *orthorhombically* distorted. The distortions can be described by strain components $\varepsilon_{xx}, \varepsilon_{yy}, \varepsilon_{zz}$ given by

$$\begin{aligned}
&[100]\text{ type}: \quad \varepsilon_{xx} = -2.75\varepsilon_0, \quad \varepsilon_{yy} = \varepsilon_0, \\
&\qquad\qquad \varepsilon_{zz} = 2.75\varepsilon_0 - \varepsilon_T, \\
&[010]\text{ type}: \quad \varepsilon_{xx} = \varepsilon_0, \quad \varepsilon_{yy} = -2.75\varepsilon_0, \\
&\qquad\qquad \varepsilon_{zz} = 2.75\varepsilon_0 - \varepsilon_T, \qquad (1) \\
&[001]\text{ type}: \quad \varepsilon_{xx} = \varepsilon_{yy} = \varepsilon_0, \quad \varepsilon_{zz} = -\varepsilon_0 - \varepsilon_T,
\end{aligned}$$

where $\varepsilon_0(-6.66 \pm 0.15) \times 10^{-4}$ at $T = 25$ K. The term ε_T is the normal thermal expansion that needs to be subtracted from ε_0 in order to obtain the true magnetostrains. Using a method devised by Morosin [15] and a Debye temperature $\Theta = 202$ K [17], and fitting the high temperature data [dashed curve in the inset in Fig. 1(b)], we obtain $\varepsilon_T = (-2.69 \pm 0.27) \times 10^{-4}$ from $T = 55$ to 25 K. We find that the thermal expansion is negligible in the x-y plane [Fig. 1(a), inset], possibly because the epitaxial film is restrained by the substrate.

The exchange striction is the result of an energy balance between the magnetoelastic energy involving spatial derivative $\nabla J(\mathbf{r})$ of the exchange interaction [11,18]

$$U_m = -2\sum_{i>j} \varepsilon_{\alpha\beta} x_\alpha \partial J(\mathbf{r}_{ij})/\partial x_\beta (\mathbf{S}_i \cdot \mathbf{S}_j), \qquad (2)$$

and the elastic energy of the crystal [1]

$$\begin{aligned}
U_e = {} & \tfrac{1}{2} C_{11}(\varepsilon_{xx}^2 + \varepsilon_{yy}^2 + \varepsilon_{zz}^2) \\
& + C_{12}(\varepsilon_{xx}\varepsilon_{yy} + \varepsilon_{yy}\varepsilon_{zz} + \varepsilon_{zz}\varepsilon_{xx}), \qquad (3)
\end{aligned}$$

where C_{11} and C_{12} are the elastic constants for a cubic crystal, the repeated indices ($\alpha, \beta = x, y, z$) imply summations, and $\mathbf{r}_{ij}$ is the position vector of the neighboring spins. To evaluate U_m, we consider up to the fourth nearest neighbors for each spin. For type-III fcc antiferromagnets, there are 8 NN AFM interactions ($\mathbf{S}_i \cdot \mathbf{S}_j = -S^2$) per chemical unit cell, all of which lie in the AFM sheets perpendicular to the unit-cell-doubling axis. These AFM bonds provide a dominant driving force for the deformation within the AFM sheets. For interactions with adjacent sheets, there are the same number of NN pairs with $\mathbf{S}_i \cdot \mathbf{S}_j = -S^2$ as those with $\mathbf{S}_i \cdot \mathbf{S}_j = +S^2$. Thus their contributions to U_m cancel completely, so that the interaction is dominated by the more distant neighbors. The total second-nearest-neighbor interactions include 4 AFM bonds along the cell-doubling direction and 8 ferromagnetic (FM) bonds within the AFM sheets. Similarly, the third nearest neighbors include 16 FM bonds, and the fourth nearest neighbors involve 8 FM bonds in, and 16 AFM bonds out of, the AFM sheets. Based on crystallographic symmetry, the magnetoelastic energy density for a [001] domain can be written as

$$U_m = (8xS^2/V_c)[B_\parallel(\varepsilon_{xx} + \varepsilon_{yy}) + B_\perp \varepsilon_{zz}], \qquad (4)$$

where x is the Mn concentration in the cation sublattice, V_c is the volume of the chemical unit cell, $S = 5/2$ for Mn, and $B_\parallel$ and $B_\perp$ are the *magnetoelastic constants*

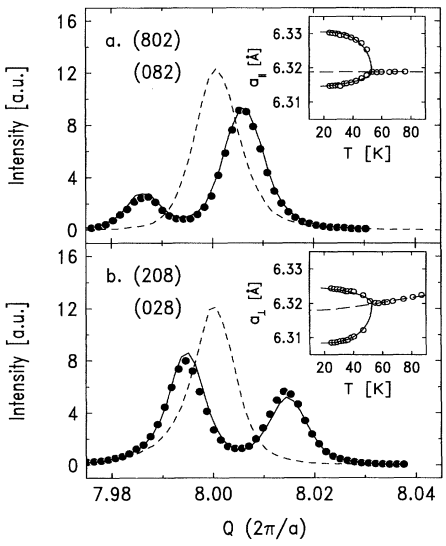

FIG. 1. X-ray diffraction peaks at $T = 25$ K for four crystallographically equivalent reflections, (802) as filled circles and (082) as solid line in (a), and (208) as filled circles and (028) as solid line in (b). The dashed lines indicate the peaks at 55 K. Insets show the temperature dependence of the lattice constants parallel ($a_\parallel$) and normal ($a_\perp$) to the thin film. The solid curves in the insets are guides to the eye, and the dashed curves are fits to the high-temperature data, indicating the behavior expected in the absence of the exchange striction.

parallel and normal to the AFM sheets, respectively, which are functions of $\nabla J(\mathbf{r})$. Equivalent forms of Eq. (4) for other types of domains are obtained by proper permutations of the strain components.

The equilibrium strain values are given by setting the derivatives of the total energy $U = U_e + U_m$ equal to a stress field (σ_x, σ_y) in the x-y plane: $\partial U/\partial \varepsilon_{xx} = -\sigma_x, \partial U/\partial \varepsilon_{yy} = -\sigma_y, \partial U/\partial \varepsilon_{zz} = 0$. This stress field retains the tetragonal symmetry for a [001] domain, but lowers the symmetry of a [100] or [010] domain to orthorhombic. Solving the above equations for the [001] or [100] domains separately, and using $C_{11} = 2C_{12} = 68$ GPa [19], together with the measured distortions in Eq. (1), we obtain $B_{\parallel} = C_s(\varepsilon_T - 1.88\varepsilon_0) = 26.1 \pm 1.5$ K and $B_{\perp} = C_s\varepsilon_T = -7.1 \pm 0.7$ K, with $C_s \equiv C_{11}V_c/8xS^2$. We note that the magnitude of $B_{\perp}$, which depends only on distant-neighbor interactions, is much smaller than that of $B_{\parallel}$ (as would be expected), but it is by no means negligible. The opposite sign of $B_{\perp}$ represents a driving force for an expansion along the cell-doubling direction, *in addition to* the usual elastic response to the contraction in the AFM sheets caused by the NN bonds. This opposite force arises mainly from the third-nearest-neighbor interactions to which a large number of FM spins contribute. This provides additional evidence for the importance of long-ranged exchange interaction among the more distant spins.

The characteristic long-range behavior cannot be explained by the existing Gaussian [7] and power-law [12] models of exchange interaction in DMS materials. In fact, forced fits by these existing models would yield $n \approx 2.3$ and a NN constant of $J_1 \approx -28$ K if the power law is used, and $\beta \approx 2.3$ and $J_1 \approx -58$ K if the Gaussian model is used.

In view of these failures we propose a new model of the spatial dependence of the superexchange interaction. There are two key parts in our new model. The first, already pointed out by Bruno and Lascaray (BL) [13], is that the superexchange interactions in DMS's do not necessarily decay monotonically as the direct distance r increases. Because the superexchange involves $3d$ electrons in Mn interacting with the p orbitals in an anion (Te), the strength of the interaction between two Mn spins depends on the number of equivalent ways that one Mn ion can connect to another Mn ion through the cation-anion-cation (CAC) chemical bonds. Based on this idea, BL suggest that $J_2 = 2J_3 = 4J_4$, where the ratios are the number of bonding connections between the neighbors. We note that the NN interaction J_1 was not included by BL in their series. The second hypothesis in our model is that the exchange interaction from one CAC bond to another is identical and independent of one another. This means that if the exchange strength of a single CAC bond, connecting two nearest neighbors, is γ, then an exchange path through two CAC bonds, connecting, e.g., the second nearest neighbors, will have the strength of γ^2. It can be seen that the new *independent-exchange-path* model predicts the following picture of the exchange constants, with J_0 being a scale factor:

$$J_1 = J_0\gamma,\ J_2 = 4J_0\gamma^2,\ J_3 = 2J_0\gamma^2,\ J_4 = J_0\gamma^2,$$
$$J_5 = 4J_0\gamma^3, \ldots . \quad (5)$$

Being the overlap integral of the neighboring-ion wave functions, γ is a function of NN separation r_0, and its physical meaning is related to the virtual hopping of a Mn-d electron between two antiparallel spin states [20].

Based on Eq. (5), the spatial gradient $\nabla J(\mathbf{r})$ is determined by the spatial derivative γ', and by the direction along which each NN exchange path is positioned. To illustrate this latter point, we consider the gradient $\nabla J_2(\mathbf{r})$ for two second nearest neighbors, i and j, along the x axis (inset in Fig. 2). The exchange coupling between these two ions consists of four equivalent pairs of NN connections (only one of such pairs is shown): $J_2 = J_0\sum_{l=1}^{4}\gamma(r_{il})\gamma(r_{lj})$. Thus, $x\partial J_2/\partial x = xJ_0\gamma\sum_{l=1}^{4}[\partial\gamma(r_{il})/\partial x + \partial\gamma(r_{lj})/\partial x] = 4J_0\gamma\gamma' r_0$. Since only two of the four NN connections are affected by strains along the y axis and along the z axis, we have $y\partial J_2/\partial y = z\partial J_2/\partial z = 2J_0\gamma\gamma' r_0$. This example demonstrates the anisotropic, directional nature of the exchange gradients, which has been taken into account in our model.

Similar evaluations of $\nabla J(\mathbf{r})$ are performed for up to the fourth nearest neighbors. Substituting these gradients in Eq. (2), we have $B_{\parallel} = r_0J_0\gamma\gamma'(1/\gamma - 8)$ and $B_{\perp} = -4r_0J_0\gamma\gamma'$. Then with the measured values of $B_{\perp}$ and $B_{\parallel}$ we obtain $\gamma = 0.0440 \pm 0.0069$ and $J_1/J_2 = 1/(4\gamma) = 5.7 \pm 0.9$, which is in good agreement with the commonly accepted values of 5–10 [8]. In fact, Eq. (5) yields the relative strengths of *all* exchange constants: J_1: J_2: J_3: J_4: J_5: ... = 5.7: 1: 1/2: 1/4: 1/23: .... As shown in Fig. 2, these values exhibit a complex decay that is

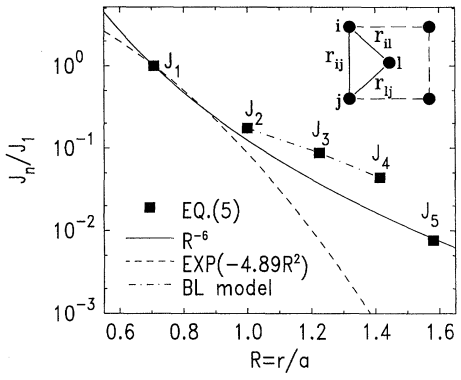

FIG. 2. Nonmonotonic spatial dependence of the Mn-Mn exchange interaction according to our independent-exchange-path model, Eq. (5), with its parameters determined from our exchange striction measurements. Also shown are calculations using several existing models. The inset shows that two second nearest neighbors, i and j, interact through consecutive nearest neighbors, i to l and l to j.

completely different from the previously discussed monotonic models. The fact that $\gamma \ll 1$ justifies our approach of omitting the more-distant-neighbor ($n \geq 5$) interactions and the higher-order bonding connections between two ions. Since within our model the parameter γ and the relative strengths of exchange constants are deduced directly from the aspect ratio $B_\perp/B_\parallel$ of the magnetoelastic distortions, they do not rely on the absolute values of the elastic or the exchange constants, making the x-ray determination very useful.

The absolute values of the exchange *derivatives*, however, *do* depend on the values of $B_\perp$ or $B_\parallel$ and of the NN exchange constant J_1. Taking $J_1 = -9.5$ K [6], we obtain $dJ_1/dr = (41 \pm 4\ \text{K})/r_0$, which gives a normalized J_1 gradient of $(r_0/J_1)dJ_1/dr = -4.3 \pm 0.4$. This agrees well with the value $-\beta = -4.89$ given by Larson *et al.* [7] in a Gaussian form $\exp(-\beta r^2/a^2)$. We would like to emphasize, however, that the *relative strengths* of the successive-neighbor interactions represent an entirely different behavior, and do not necessarily follow the Gaussian dependence, as shown in Fig. 2.

As we mentioned earlier, the exchange striction which we observe occurs at a temperature well below the Neél temperature for the AFM transition. This delayed effect can be explained by the residual stress (σ_x, σ_y) in the $Zn_{1-x}Mn_xTe$ epilayer. Using the observed distortions in Eq. (1), we obtain an isotropic stress field $\sigma_x = \sigma_y = -C_{11}(\varepsilon_T - 1.75\varepsilon_0)/2 = -30$ MPa for all three types of domains. This compressive stress creates an energy barrier $-\sigma\,\Delta A$ for the [100] and [010] domains because of their area dilation $\Delta A = \varepsilon_{xx} + \varepsilon_{yy} = -1.75\varepsilon$ ($\varepsilon < 0$). Thus a contraction within the AFM sheets in these domains does not lower the free energy unless the average spin alignment $\langle S^2 \rangle$ is above a certain threshold, causing the striction to occur at a temperature lower than the Néel point as observed in the experiment. Although the [001] domains do not have this threshold, the existence of the substrate restrains the sample's physical dimensions, causing all three types of domains to form at the same temperature.

Our findings have important implications to the basic understanding of DMS materials. Contrary to most theoretical studies where the effect of magnetoelastic energy has been ignored, our result indicates that this effect, which gives rise to an effective biquadratic isotropic exchange, is of the same order of magnitude as some theoretically predicted values of weak interactions, such as the anisotropic DM exchange [21]. It may therefore play an important part in theories dealing with such weak interactions. The effective biquadratic term may influence various magnetic spectroscopic measurements, such as electron paramagnetic resonance [20,22]. The measured value of the NN exchange gradient dJ_1/dr provides essential information for quantitative analyses of other magnetoelastic effects, such as the strain-induced helimagnetism in the molecular-beam-epitaxy-grown DMS multilayers [23]. Finally, our new independent-exchange-path model, Eq. (5), provides a unified picture of the spatial dependence of $J(r)$, and may stimulate further theoretical studies in this area as well as further experimental research on magnetization steps, low-temperature susceptibility, and neutron scattering.

We acknowledge helpful discussions with M. Sutton and C. Henley. This work is supported by NSF through CHESS under Grant No. DMR9311772. The work at Notre Dame is supported by NSF/MRG Grant No. DMR9221390.

*Present address: Department of Physics and Astronomy, State University of New York at Buffalo, Amherst, NY 14260.

[1] C. Kittel, *Introduction to Solid State Physics* (Wiley, New York, 1956), 2nd ed.
[2] J. K. Furdyna, J. Appl. Phys. **64**, R29 (1988).
[3] T. M. Giebultowicz and T. M. Holden, in *Semiconductors and Semimetals,* edited by J. K. Furdyna and J. Kossut (Academic, Boston, 1988), Vol. 25.
[4] Y. Shapira, J. Appl. Phys. **67**, 5090 (1990).
[5] L. M. Corliss *et al.,* Phys. Rev. B **33**, 608 (1986).
[6] T. M. Giebultowicz, J. J. Rhyne, and J. K. Furdyna, J. Appl. Phys. **61**, 3537 (1987).
[7] B. E. Larson *et al.,* Phys. Rev. B **37**, 4137 (1988).
[8] W. J. M. de Jonge and H. J. M. Swagten, Magn. Magn. Mater. **100**, 322 (1991).
[9] T. Q. Vu *et al.,* Phys. Rev. B **46**, 11 617 (1992).
[10] C. L. Henley, Phys. Rev. Lett. **62**, 2056 (1989).
[11] B. E. Larson and C. L. Henley (to be published).
[12] A. Twardowski *et al.,* Phys. Rev. B **36**, 7013 (1987).
[13] A. Bruno and J. P. Lascaray, Phys. Rev. B **38**, 9168 (1988).
[14] S. Greenwald and J. S. Smart, Nature (London) **166**, 523 (1950).
[15] B. Morosin, Phys. Rev. B **1**, 236 (1970).
[16] T. M. Giebultowicz *et al.,* Phys. Rev. B **48**, 12 817 (1993).
[17] S. Oseroff and P. H. Keesom, in *Semiconductors and Semimetals,* edited by J. K. Furdyna and J. Kossut (Academic, Boston, 1988), Vol. 25.
[18] E. Callen, J. Appl. Phys. **39**, 519 (1968).
[19] $C_{11} \approx 2C_{12}$ is taken from J. R. Buschert *et al.,* Phys. Rev. B **49**, 4619 (1994). $C_{11} = 60$ GPa at room temperature is taken from E. Abramof *et al.,* Appl. Phys. Lett. **64**, 49 (1994). This value is then multiplied by 1.14 to yield $C_{11} = 68$ GPa at 20 K, using a universal linear temperature dependence given by R. Fürth [Proc. Cambridge Philos. Soc. **37**, 34 (1941).
[20] E. A. Harris, J. Phys. C **5**, 338 (1972).
[21] T. Moriya, in *Magnetism,* edited by G. T. Rado and H. Suhl (Academic, New York, 1963), Vol. 1.
[22] B. E. Larson and H. Ehrenreich, Phys. Rev. B **39**, 1747 (1989); J. Appl. Phys. **67**, 5084 (1990).
[23] T. M. Giebultowicz *et al.,* Phys. Rev. B **46**, 12 076 (1992).